International Nano Letters
a SpringerOpen Journal

ORIGINAL ARTICLE Open Access

Preparation and characterization of SnO_2 nanoparticles by hydrothermal route

Ganesh E Patil[1], Dnyaneshwar D Kajale[2], Vishwas B Gaikwad[1] and Gotan H Jain[1*]

Abstract

This paper demonstrates the synthesis of SnO_2 nanoparticles using a simple hydrothermal route in the presence of the surfactant hydrazine at 100 °C for 12 h. X-ray diffraction (XRD), field emission scanning electron microscopy, and transmission electron microscopy (TEM) were employed to characterize the as-prepared product, and optical property was studied by UV-visible diffuse reflectance spectroscopy (DRS). The XRD pattern of the as-prepared sample is indexed to the tetragonal structure of SnO_2, and the calculated particle size is 22.4 nm, which is further confirmed by TEM. The selected area electron diffraction patterns showed continuous ring patterns without any additional diffraction spots and rings of secondary phases, revealing their crystalline structure. Analysis of the DRS spectrum showed the bandgap of the synthesized SnO_2 to be 3.6 eV. The anionic surfactant hydrazine plays a key role in the formation of the SnO_2 nanostructures. A probable reaction for the formation of SnO_2 nanoparticles is proposed.

Keywords: SnO_2 nanoparticles, Hydrothermal route, FESEM, TEM

Background

Nanomaterials have attracted great interest due to their intriguing properties, which are different from those of their corresponding bulk state. In the past few years, SnO_2 is an important n-type wide-energy-gap semiconductor (Eg = 3.64 eV, 330 K) which has a wide range of applications such as in solid-state gas sensors [1], transparent conducting electrodes [2], rechargeable Li batteries [3], and optical electronic devices [4]. During the past decade, SnO_2 nanostructures have been one of the most important oxide nanostructures due to their properties and potential applications [5,6].

Many processes have been developed to the synthesis of SnO_2 nanostructures, e.g., spray pyrolysis [5], hydrothermal methods [6-8], evaporating tin grains in air [9], chemical vapor deposition [10], thermal evaporation of oxide powders [11], rapid oxidation of elemental tin [12], the sol–gel method [13], etc. Davar et al. [14] reported the synthesis of SnO_2 nanoparticles by thermal decomposition using [bis(2-hydroxyacetophenato)tin(II)], $[Sn(HAP)_2]$, as precursor. Salavati-Niasari et al. [15] synthesized zinc blend ZnS nanoparticles by a thioglycolic acid ($HSCH_2COOH$)-assisted hydrothermal technique via the reaction between a new inorganic precursor [bis(2-hydroxyacetophenato)zinc(II)], $[Zn(HAP)_2]$, and thioacetamide (CH_3CSNH_2). Gnanam and Rajendran [16] synthesized nanocrystalline tin oxide powders of about 8 to 13 nm in size using different surfactants such as cetyltrimethyl ammonium bromide, sodium dodecyl sulphate, and polyethylene glycol via hydrothermal reaction at 160°C for 12 h and studied their structural and photoluminescence properties.

A simple hydrazine-assisted hydrothermal route was employed to synthesize nanocrystalline SnO_2 powders in this study, and structural, morphological, microstructural, and optical properties were discussed.

Methods

All reagents used were of analytical grade without further purification. First, 3.505 g of $SnCl_4{\cdot}5H_2O$ (0.1 M) was dissolved in 100 ml of distilled water, and then 1.2800 g of hydrazine hydrate (0.01 M) was added with stirring. $N_2H_4{\cdot}H_2O$ immediately reacted with $SnCl_4$ in the solution to form a slurry-like white precipitate of the hybrid complex between N_2H_4 and $SnCl_4$. After 10 min of stirring, the solution was transferred into a Teflon-lined stainless steel autoclave with a capacity of 200 ml

* Correspondence: gotanjain@rediffmail.com
[1]Materials Research Laboratory, K.T.H.M. College, Nashik 422 002, India
Full list of author information is available at the end of the article

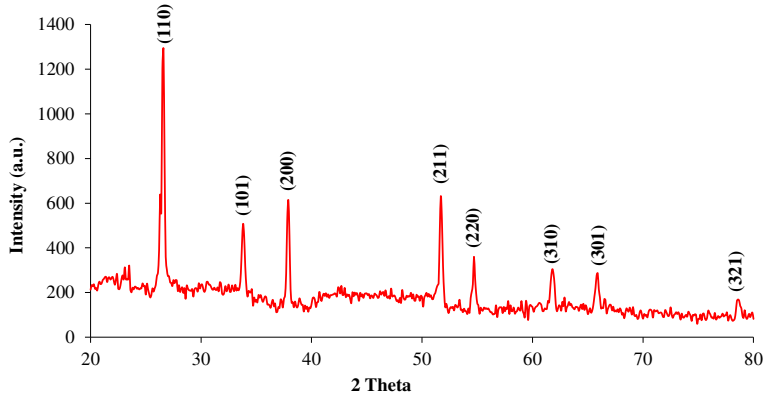

Figure 1 XRD pattern of the SnO_2 sample.

and then sealed. The autoclave was maintained at 100°C for 12 h and cooled naturally to room temperature. The product was centrifuged, filtered out, and rinsed with methanol and distilled water several times, and then dried at 120°C for 1 h in air.

The possible reaction of $SnCl_4{\cdot}5H_2O$ with hydrazine produced SnO_2 nanoparticles via Sn^{4+} reaction with NH_4OH. The process can be expressed as follows:

$$m\mathrm{SnCl_4} + n\mathrm{N_2H_4} \rightarrow (\mathrm{SnCl_4})_m(\mathrm{N_2H_4})_n \quad (1)$$

$$(\mathrm{SnCl_4})_m(\mathrm{N_2H_4})_n \rightarrow m\mathrm{Sn^{4+}} + n\mathrm{N_2H_4} + 4m\mathrm{Cl^-} \quad (2)$$

$$3\mathrm{N_2H_4} + 4\mathrm{H_2O} \rightarrow 4\mathrm{NH_4OH} + \mathrm{N_2} \quad (3)$$

$$\mathrm{Sn^{4+}} + 4\mathrm{NH_4OH} \rightarrow \mathrm{SnO_2}\downarrow + 4\mathrm{NH_4^+} + 2\mathrm{H_2O}. \quad (4)$$

Prior to the hydrothermal process, the $(SnCl_4)_m(N_2H_4)_n$ complex clusters were formed via reaction (1), and at the same time, the clusters were agglomerated into the slurry-like white precipitate mentioned above. As represented in reaction (2), the $(SnCl_4)_m(N_2H_4)_n$ clusters underwent dissociation when the solution was heated to 100°C during the hydrothermal stage. In reaction (3), OH^- ions were formed via the dissociation of N_2H_4 into NH_4OH and N_2 [17]. Reaction (4) represents the formation of the SnO_2 nanoparticles via the reaction between Sn^{4+} and OH^- ions formed in reaction (3).

The synthesized sample was characterized by X-ray powder diffraction (XRD) using the XRD Make-Bruker D-8 model (Bruker AXS, Inc., Madison, WI, USA) with CuKα radiation with a wavelength λ =1.5418 Å at 2θ values between 20° and 80°. Transmission electron microscopy (TEM) images were recorded from a transmission electron microscope (CM-200, Make-PHILIPS, Amsterdam, The Netherlands). The UV-visible (UV–vis) diffuse reflectance spectrum (DRS) was obtained from a JASCO UV–vis/NIR spectrophotometer V-670 model (Easton, MD, USA).

Results and discussion

Structural properties by XRD

The XRD pattern of the product is shown in Figure 1. The peaks at 2θ values of 26.6°, 33.8°, 37.9°, 51.8°, 54.7°,

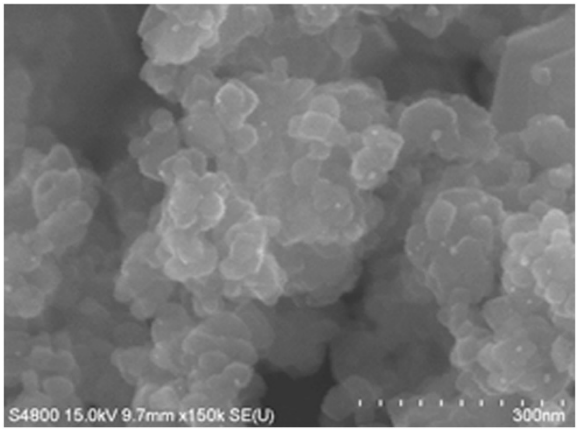

Figure 2 FESEM image of the SnO_2 sample.

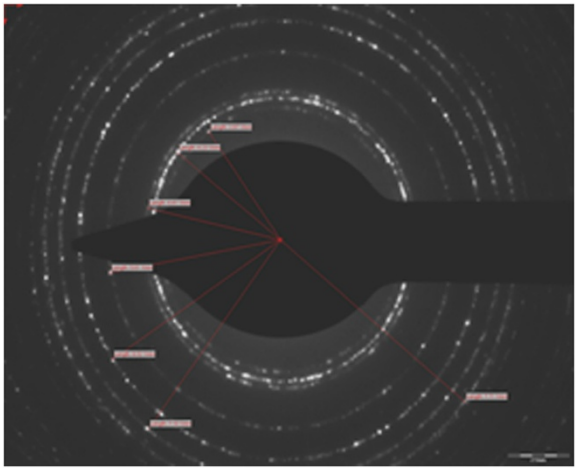

Figure 3 SAED pattern of the SnO_2 sample.

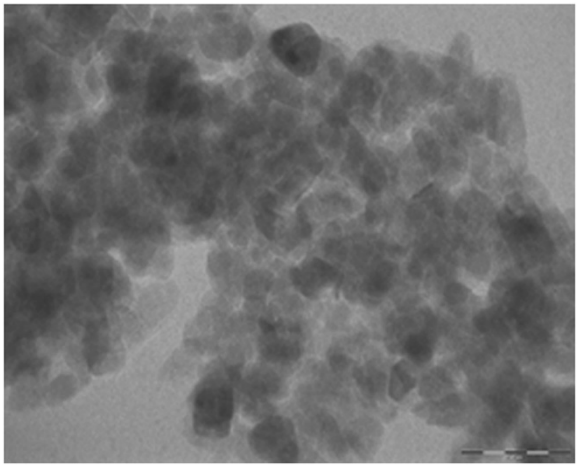

Figure 4 TEM image of the SnO_2 sample.

61.9°, and 65.9° can be associated with (1 1 0), (1 0 1), (2 0 0), (2 1 1), (2 2 0), (3 1 0), and (3 0 1), respectively. A matching of the observed and standard (*hkl*) planes confirmed that the product is of SnO_2 having a tetragonal structure, which are in good agreement with the literature values (JCPDS card no. 41–1445). The average particle size (D) was estimated using the Scherrer equation [18]:

$$D = \frac{0.9\lambda}{\beta \cos\theta}, \tag{5}$$

where D is the crystallite size, λ is the X-ray wavelength, β is the full width at half maximum of the diffraction peak, and θ is the Bragg diffraction angle of the diffraction peaks. The average particle size was found to be 22.4 nm.

Morphological properties by FESEM

Figure 2 shows the field emission scanning electron microscopy (FESEM) micrograph of the synthesized SnO_2 sample. Clustering of particles seems to have occurred on the surface. In this image, cubic structures can be easily seen.

Microstructural properties by TEM and SAED pattern

Figure 3 shows the electron diffraction patterns of the sample. It is clear from the figure that the SnO_2 particles are crystalline in nature. The electron diffraction patterns show continuous ring patterns without any additional diffraction spots and rings of secondary phases, revealing their crystalline structure. Seven fringe patterns corresponding to planes (1 1 0), (1 0 1), (2 0 0), (2 1 1), (2 2 0), (3 1 0), and (3 0 1) are consistent with the peaks observed in the XRD patterns. XRD and TEM studies confirmed pure tetragonal structure of SnO_2 as evidenced from Figures 1 and 4, respectively. The ring-to-the-center distance of each ring is measured as 3.01, 4.23, 4.41, 5.61, 6.52, 7.10, and 7.71 and expressed in terms of nm^{-1}. The reciprocal of these values gives the interplanar distance d. Details are given in Table 1.

Optical properties by UV–vis DRS

To determine the optical bandgap of synthesized SnO_2, the reflectance spectra of the SnO_2 thick film prepared by screen printing technique [19] on a glass substrate was measured. The reflectance (R) spectra of the SnO_2 thin film were shown in Figure 5.

As seen in Figure 5, the reflectance spectra show a strong decrease after 360 nm. This decrease is related to optical transitions occurring in the optical bandgap. In order to determine the precise value of the optical bandgap of the SnO_2, the reflectance values were converted to absorbance by application of the Kubelka-Munk function [20,21].

The Kubelka-Munk theory is generally used for the analysis of diffuse reflectance spectra obtained from weakly absorbing samples. The Kubelka-Munk formula is expressed by the following relation:

$$F(R) = \frac{(1-R)^2}{2R} = \frac{K}{S}, \tag{6}$$

where $F(R)$ is the Kubelka-Munk function which corresponds to the absorbance, R is the reflectance, K is the absorption coefficient, and S is the scattering coefficient.

Table 1 *d* values obtained from XRD and TEM

Reported *d* values (Å)	XRD *d* values (Å)	Electron diffraction (TEM)		Planes (*hkl*)
		Reciprocal of *d* values δ_{hkl} (nm^{-1})	*d* values d_{hkl} (Å)	
3.35	3.342	3.01	3.320	(1 1 0)
2.64	2.604	4.23	2.364	(1 0 1)
2.37	2.372	4.41	2.267	(2 0 0)
1.76	1.770	5.61	1.782	(2 1 1)
1.67	1.653	6.52	1.533	(2 2 0)
1.50	1.501	7.10	1.408	(3 1 0)
1.41	1.418	7.71	1.297	(3 0 1)

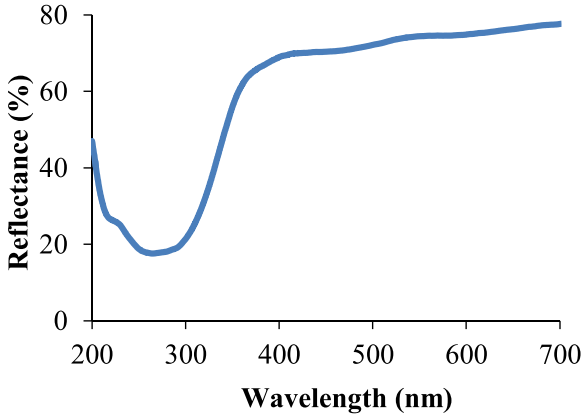

Figure 5 Reflectance spectra of the SnO_2 thin film.

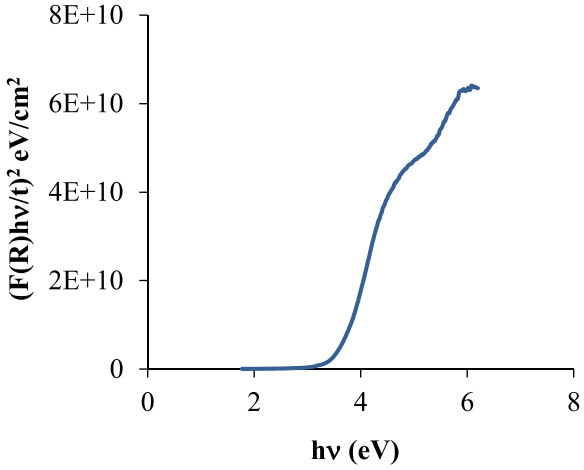

Figure 6 Plot of $(\alpha h\nu)^2$ vs. hν for the SnO_2 thin film.

It is well known that the optical transitions in semiconductor materials are taken place by direct and indirect transitions. The absorption coefficient α for direct transitions is expressed by the following relation [22]:

$$\alpha h\nu = A(h\nu - Eg)^n, \quad (7)$$

where α is the linear absorption coefficient of the material, A is an energy-independent constant, Eg is the optical bandgap, and n is a constant which determines the type of optical transitions: for indirect allowed transition, $n = 2$; for indirect forbidden transition, $m = 3$; for direct allowed transition, $n = 1/2$; and for direct forbidden transition, $m = 3/2$. The $F(R)$ values of the SnO_2 film were obtained using the $\frac{(1-R)^2}{2R}$ relation in Equation 6 [23,24] and the Kubelka-Munk function $F(R)$ is directly proportional to the absorbance. Therefore, $F(R)$ values were converted to the linear absorption coefficient by means of the $\alpha = \frac{F(R)}{t} = \frac{\text{Absorbance}}{t}$ relation [25], where t is the thickness of the SnO_2 film. The curve of $\left(\frac{F(R)h\nu}{t}\right)^2$ vs. hν for the SnO_2 film was plotted, as shown in Figure 6. The optical bandgap (Eg) of the SnO_2 film was determined from the curve of $\left(\frac{F(R)h\nu}{t}\right)^2$ vs. hν and was found to be 3.6 eV. The optical bandgap of the SnO_2 studied is similar to that of undoped SnO_2 materials obtained by various methods [26,27]. This suggests that the optical bandgap of SnO_2 semiconductors changes with respect to the synthesis method used.

Conclusions

SnO_2 nanoparticles have been successfully synthesized by a simple hydrothermal method at low temperature using hydrazine hydrate as a mediator. The structural, morphological, microstructural, and optical properties of a SnO_2 sample were investigated. XRD spectra indicated that the as-prepared product is polycrystalline in nature. It was also shown from these spectra that the crystallite structure was observed to be tetragonal. The surface morphology was investigated by FESEM. The crystallite size (22.4 nm) of the SnO_2 nanoparticles, estimated by XRD, is confirmed by TEM. The optical bandgap of the SnO_2 film was found to be 3.6 eV.

Competing interests

The authors declare that they have no competing interests.

Authors' contributions

GEP synthesized the nanocrystalline SnO_2 materials, carried out the characterization, and drafted the manuscript. DDK participated in the discussions and interpretation of all characterization results. VBG and GHJ gave the final approval of the version to be published. All the authors read and approved the final manuscript.

Authors' information

GEP is an INSPIRE fellow at Materials Research Laboratory, KTHM College, Nashik, India. He received his B.Sc. and M.Sc. (Physics) degrees from North Maharashtra University, Jalgaon, in 2005 and 2007, respectively. He is currently pursuing a Ph.D. degree under the supervision of Dr. GHJ at the University of Pune, Pune. He is a life member of the Indian Science Congress Association. His research interests are in the areas of preparation of binary oxide thin film by spray pyrolysis and its gas sensing applications.

DDK is an assistant professor at MVP's Arts, Commerce and Science College, Nandgaon, India. He received his B.Sc. and M.Sc. (Chemistry) degrees from the University of Pune. He has 25 peer-reviewed research publications to his credit. He is a life member of the Indian Science Congress Association. His research interest is in the areas of perovskite materials for gas sensors, thin films, and nanosized material preparation.

Dr. VBG received his M.Sc., M.Phil., and Ph.D. degrees from the University of Pune, Pune, in 1981, 1990, and 2001, respectively. He is currently a professor and the Head of the KTHM College, Nashik, and a member of the Management Council, University of Pune. His research interest is in the areas of environmental science, material science, and nanomaterials. He is a member of the Indian Association of Nuclear Chemists and Allied Scientists, BARC, Mumbai.

Dr. GHJ is an associate professor and the Head of the Department of Physics at MVP's KTHM College, Nashik, India. He received his M.Sc. (Physics) degree from the University of Pune, Pune, in 1989 and Ph.D. (Materials Science) degree from Pratap College, Amalner, North Maharashtra University, Jalgaon, in 2007. He has published 44 research articles in the Journal of International Repute. His areas of interest are perovskite for gas sensors, nanomaterials, and thick and thin films. He has

delivered invited talks at MS&T 2008, USA; EUROMAT 2009, UK; ICST 2010, Italy; ICST 2011, New Zealand; and ICPAC-2012, Mauritius. He is a BOS member in Physics at the University of Pune, Pune.

Acknowledgements
The financial support for this work through the INSPIRE Fellowship for doctoral degree from DST, New Delhi, is gratefully acknowledged. The authors thank the Sophisticated Analytical Instrument Facility, Indian Institute of Technology (IIT), Bombay, for carrying out TEM characterization and C-MET, Pune, for providing the FESEM facility.

Author details
[1]Materials Research Laboratory, K.T.H.M. College, Nashik 422 002, India.
[2]Materials Research Laboratory, Arts, Commerce and Science College, Nandgaon 423 106, India.

Received: 1 April 2011 Accepted: 28 February 2012
Published: 27 July 2012

References

1. Ying, Z., Wan, Q., Song, Z.T., Feng, S.L.: SnO_2 nanowhiskers and their ethanol sensing characteristics. Nanotechnology **15**, 1682 (2004)
2. Chopra, K.L., Major, S., Pandya, D.K.: Transparent conductors–a status review. Thin Solid Films **102**, 1 (1983)
3. Peng, Z., Shi, Z., Liu, M.: Mesoporous Sn–TiO_2 composite electrodes for lithium batteries. Chem. Commun. **21**, 25 (2000)
4. Aoki, A., Sasakura, H.: Tin oxide thin film transistors. Japan J. Appl. Phys. **9**, 582 (1970)
5. Paraguay-Delgado, F., Antúnez-Flores, W., Miki-Yoshida, M., Aguilar-Elguezabal, A., Santiago, P., Diaz, R., Ascencio, J.A.: Structural analysis and growing mechanisms for long SnO_2 nanorods synthesized by spray pyrolysis. Nanotechnology **16**, 688 (2005)
6. Cheng, B., Russell, J.M., Shi, W., Zhang, L., Samulski, E.T.: Large-scale, solution-phase growth of single-crystalline SnO_2 nanorods. J. Am. Chem. Soc. **126**, 5972 (2004)
7. Du, F., Guo, Z., Li, G.: Hydrothermal synthesis of SnO_2 hollow microspheres. Mater. Lett. **59**, 2563 (2005)
8. Fujihara, S., Maeda, T., Ohgi, H., Hosono, E., Imai, H., Kim, S.: Hydrothermal routes to prepare nanocrystalline mesoporous SnO_2 having high thermal stability. Langmuir **20**, 6476 (2004)
9. Duan, J., Yang, S., Liu, H., Gong, J., Huang, H., Zhao, X., Zhang, R., Du, Y.: Single crystal SnO_2 zigzag nanobelts. J. Am. Chem. Soc. **127**, 6180 (2005)
10. Liu, Y., Koep, E., Liu, M.: A highly sensitive and fast-responding SnO_2 sensor fabricated by combustion chemical vapor deposition. Chem Mater **17**, 3997 (2005)
11. Dai, Z.R., Gole, J.L., Stout, J.D., Wang, Z.L.: Tin oxide nanowires, nanoribbons, and nanotubes. J. Phys. Chem. B **106**, 1274 (2002)
12. Hu, J.Q., Ma, X.L., Shang, N.G., Xie, Z.Y., Wong, N.B., Lee, C.S., Lee, S.T.: Large scale rapid oxidation synthesis of SnO_2 nanoribbons. J. Phys. Chem. B **106**, 3823 (2002)
13. Pourfayaz, F., Khodadadi, A., Mortazavi, Y., Mohajerzadeh, S.S.: SnO_2 sensor selective to ethanol in presence of CO, LPG and CH_4. Sensors Actuators B **108**, 172 (2005)
14. Davar, F., Salavati-Niasaria, M., Fereshteh, Z.: Synthesis and characterization of SnO_2 nanoparticles by thermal decomposition of new inorganic precursor. J. Alloys Compd. **496**(1–2), 638–643 (2010)
15. Salavati-Niasari, M., Davar, F., Seyghalkar, H., Esmaeili, E., Mir, N.: Synthesis and characterization of SnO_2 nanoparticles by thermal decomposition of new inorganic precursor. Cryst. Eng. Comm. **13**, 2948 (2011)
16. Gnanam, S., Rajendran, V.: Anionic, cationic and nonionic surfactants-assisted hydrothermal synthesis of tin oxide nanoparticles and their photoluminescence properties. Digest Journal of Nanomaterials and Biostructures **5**(2), 623 (2010)
17. Zhu, H., Yang, D., Yu, G., Zhang, H., Yao, K.: Hydrothermal synthesis of Zn_2SnO_4 nanorods in the diameter regime of sub-5 nm and their properties. Nanotechnology **17**, 2386 (2006)
18. Cullity, B.D.: Elements of X-ray Diffraction. Boston, Addison-Wesley Publishing Co (1956)
19. Jain, G.H., Patil, L.A., Wagh, M.S., Patil, D.R., Patil, S.A., Amalnerkar, D.P.: Surface modified $BaTiO_3$ thick film resistors as H_2S gas sensors. Sensors Actuators B Chemical **117**, 159 (2006)
20. Escobedo Morales, A., Sanchez Mora, E., Pal, U.: Use of diffuse reflectance spectroscopy for optical characterization of un-supported nanostructures. Rev. Mexic. De Fisica S **53**, 18 (2007)
21. Senthilkumar, V., Vickraman, P., Ravikumar, R.: Synthesis fluorine doped tin oxide nanoparticles by sol–gel technique and characterization. Journal of Sol–gel Science and Technology **53**(2), 316 (2010)
22. Caglar, M., Ilican, S., Caglar, Y., Yakuphanoglu, F.: The effects of Al doping on the optical constants of ZnO thin films prepared by spray pyrolysis method. Int. J. Mater. Sci. Elect. Res. **1**, 21 (2010)
23. Caglar, M., Ilican, S., Caglar, Y., Yakuphanoglu, F.: Electrical conductivity and optical properties of ZnO nanostructured thin film. Appl. Surf. Sci. **255**, 4491 (2009)
24. Liu, X.-C., Shi, E.-W., Chen, Z.-Z., Zhang, H.-W., Song, L.-X., Wang, H., Yao, S.-D.: Structural, optical and magnetic properties of co-doped ZnO films. J. Cryst. Growth **296**, 135 (2006)
25. Silva, R.F., Darbello Zaniquelli, M.E.: Aluminium doped zinc oxide films: formation process and optical properties. J. Non-Cryst. Solids 1**247**, 248 (1999)
26. Patil, G.E., Kajale, D.D., Ahire, P.T., Chavan, D.N., Pawar, N.K., Shinde, S.D., Gaikwad, V.B., Jain, G.H.: Synthesis, characterization and gas sensing performance of SnO_2 thin films prepared by spray pyrolysis. Bull. Mater. Sci. **120**, 1 (2011)
27. Patil, G.E., Kajale, D.D., Gaikwad, V.B., Jain, G.H.: Nanocrystalline tin oxide thin film as a low level H_2S gas sensor. Int. J. Nanosci. **10**, 1 (2011)

doi:10.1186/2228-5326-2-17
Cite this article as: Patil *et al.*: **Preparation and characterization of SnO_2 nanoparticles by hydrothermal route.** *International Nano Letters* 2012 **2**:17.